Biochemistry

 Volume 40, Number 5 February 6, 2001

Articles

Anti-gene Effect in Live Cells of AG Motif Triplex-Forming Oligonucleotides Containing an Increasing Number of Phosphorothioate Linkages[†]

Susanna Cogoi,[‡] Valentina Rapozzi,[‡] Franco Quadrifoglio,[‡,§] and Luigi Xodo*[,‡,§]

Department of Biomedical Sciences and Technologies and Department of Bone Marrow Transplantation, School of Medicine, University of Udine, Piazzale Kolbe 4, 33100 Udine, Italy

Received June 1, 2000; Revised Manuscript Received November 30, 2000

ABSTRACT: The murine Ki-*ras* promoter contains a unique polypurine−polypyrimidine [poly(R·Y)] sequence between −290 and −320 from the 3′ boundary of exon ϕ. Previously we demonstrated triplex formation and transcription inhibition promoted by GT and AG oligonucleotides directed against this site [Alunni-Fabbroni et al. (1996) *Biochemistry 35*, 16361−16369]. In this work, we have investigated triplex formation and anti-gene activity of five 20-mer AG motif triplex-forming oligonucleotides specific for the Ki-*ras* poly(R·Y) target, derived from 5′-AGGGAGGGAGGAAGGGAGGG (20AG) by replacing an increasing number of phosphodiester linkages with phosphorothioate linkages (S_i-20AG; $i = 2, 3, 4, 5, 19$). Electrophoretic mobility-shift experiments (EMSA) showed that four thioate oligonucleotides, S_i-20AG ($i = 2, 3, 4, 5$), recognized the Ki-*ras* target and exhibited dissociation constants similar to that of 20AG: $K_d = 12 \pm 2$ nM, while the all-thioate S_{19}-20AG exhibited a K_d of 128 ± 15 nM. Moreover, the binding between the Ki-*ras* promoter and oligonucleotides S_i-20AG ($i = 2, 3, 4, 5, 19$) was characterized by DMS/piperidine and DNase I footprinting experiments. We observed that the introduction in the phosphodiester oligonucleotide 20AG of sulfur atoms reduced its aggregation significantly and increased its nuclease resistance. Transient transfection experiments using preformed triplexes with a recombinant plasmid containing the reporter chloramphenicol acetyltransferase (CAT) gene under the control of Ki-*ras* promoter showed that oligonucleotides S_i-20AG ($i = 2, 3, 4, 5, 19$) promote a strong inhibition of up to 75% of the CAT expression when compared with control Ki-*ras* unspecific oligonucleotides. Taken together, these data provide a guideline for designing triplex-forming effector molecules capable of controlling Ki-*ras* expression in vivo.

Phosphorothioate oligonucleotides (S-ODNs)[1] are DNA analogues in which a number of natural phosphorodiester backbone linkages are modified into phosphorothioate analogues. As these compounds are less susceptible to degradation by cellular nucleases, they have been widely employed in antisense strategy (*1*). A number of S-ODNs have indeed reached phase I and phase II in clinical trials for the treatment

[†]This work was supported by the Italian Ministry of Scientific Research (Cofin 98) and the University of Udine.

* To whom correspondence should be addressed at the Department of Biomedical Sciences and Technologies, School of Medicine, Piazzale Kolbe, 4, University of Udine, 33100 Udine, Italy. Tel (+39)(432)-(49.4395); Fax (+39)(432)(49.4301); email: lxodo@makek.dstb.uniud.it.

[‡] Department of Biomedical Sciences and Technologies.

[§] Department of Bone Marrow Transplantation.

[1] Abbreviations: S-ODN, phosphorothioate oligonucleotide; DMS, dimethyl sulfate; poly(R·Y), polypyrimidine−polypurine; CAT, chloramphenicol acetyltransferase; EMSA, electrophoresis mobility shift assay; 293 cells, embryonic kidney cell line.

10.1021/bi0012639 CCC: $20.00
Published on Web 01/12/2001

of cancer and viral infections (*2*). Although the use of antisense oligonucleotides has proved to be efficacious in several clinical studies, some problems remain to be solved, such as a restricted accessibility to the target, due to the intrinsic structure of mRNA, and unwanted nonantisense effects.

As S-ODNs maintain the property of binding to the double helix of DNA via triple-helix formation, they can be employed as transcription repressors in anti-gene strategies (*3, 4*). Previous studies showed that the sulfurization of the third strand in pyrimidine motif triplexes (parallel triplexes) results in a destabilization of triplex DNA (*5*−*8*). In particular, it was reported that the higher the number of phosphorothioate linkages introduced in the third strand, the more pronounced is the destabilization of the triplex (*8*). However, in the case of purine motif triplexes (antiparallel triplexes), the sulfur atoms seem to have a different effect. Dervan and co-workers reported that all-thioate purine-rich oligonucleotides bind to duplex DNA with an affinity greater than that of all-thioate pyrimidine oligonucleotides (*9*). It has also recently been reported that the stability of triplexes formed by purine S-ODNs is comparable to that of the phosphodiester analogues (*10, 11*).

In the present study, we wished to investigate both the binding property and the anti-gene capacity in cultured cells of a number of AG motif triplex-forming oligonucleotides containing an increasing number of phosphorothioate linkages. The DNA target used for this study is a unique poly(R·Y) sequence of 30 base pairs present in the promoter of the murine Ki-*ras* oncogene. Both target and S-ODNs are shown in Figure 1. The S-ODNs were derived from oligonucleotide 5′-AGGGAGGGAGGAAGGGAGGG, termed 20AG, by replacing certain phosphodiester linkages with phosphorothioate linkages. In earlier work, we have demonstrated that 20AG and its GT analogue inhibit the transcription both in vitro (*12*) and in vivo (*13*).

The substitution of a nonbridging oxygen with a sulfur atom introduces a chiral center in each phosphorothioate linkage, with the consequence that two stereoisomers, R_p and S_p, are generated by each internucleotide phosphorothioate group. As the automated solid-phase synthesis of S-ODNs is not stereospecific, the designed S-ODNs for the Ki-*ras* target exist in solution as a mixture of 2^{n-1} distereoisomers (where *n* is the number of phosphorothioate linkages present in the oligonucleotide). Enzymatic synthesis of pure S-ODN stereoisomers is not convenient, in particular for producing large oligonucleotide quantities necessary for biological experiments.

Here, we show that nonstereospecific S-ODNs, with the same AG motif sequence but containing different levels of phosphorothioate modifications, form very stable triple helices with a unique poly(R·Y) target of Ki-*ras* and also exhibit a remarkable anti-gene capacity as they strongly repress the expression of the reporter CAT gene, placed under the control of the Ki-*ras* promoter, in 293 cultured cells.

MATERIALS AND METHODS

Oligodeoxynucleotides. The oligodeoxynucleotides used in this study were synthesized using a standard phosphoroamidite solid-phase chemistry on a Beckman Oligo 1000 DNA synthesizer. The deprotected oligonucleotides were purified by FPLC anion exchange chromatography, using a MONO Q column, eluted with a linear gradient of ammonium bicarbonate. The oligonucleotides used for the footprinting experiments were purified by electrophoresis (*14*). Sample purity was checked by 20% PAGE in the presence of 7 M urea. The samples were lyophilized and stored at −20 °C. Oligonucleotide concentrations of stock solutions in Milli Q water were determined by UV spectroscopy using as extinction coefficients at 260 nm 7500, 8500, 15 000, and 12 500 M^{-1} cm^{-1} for C, T, A, and G, respectively.

Plasmids. Plasmid pKRS-413 used for the transient transfection experiments was generously supplied by D. George (University of Pennsylvania). Its structure has been previously reported (*15*). Briefly, it derives from vector pSVAOcat in which a 380 bp segment of the Ki-*ras* promoter capable of driving transcription was cloned. A promoterless CAT gene was inserted downstream from the Ki-*ras* promoter. This construct is able to drive CAT transcription in a host cell (*13*). Plasmid pTK β-gal, used to determine transfection efficiency, was purchased from Promega Biosciences (San Luis Obispo, CA).

Circular Dichroism Spectra. Circular dichroism (CD) spectra were recorded on a Jasco 600 A spectropolarimeter, equipped with a temperature-regulated cuvette holder. The spectra were recorded using a 5 mm path length quartz cuvette containing a DNA solution at a concentration of 3 μM. The CD spectra shown are the average of four accumulations from which the baseline was subtracted. The CD spectra report on the ordinate the ellipticity in millidegree units.

Electrophoresis Mobility Shift Experiments (EMSA) and Footprinting. EMSA experiments were performed using as target a synthetic 60-mer duplex containing the poly(R·Y) sequence of Ki-*ras* (Figure 1). The duplex was prepared by annealing (30 min at 60 °C, 2 h at 37 °C, and overnight incubation at room temperature) the purine strand, end-labeled with [γ-^{32}P]ATP and T4 polynucleotide kinase, with the complementary pyrimidine strand. The labeled Ki-*ras* duplex was passed through a Sephadex G50 column to remove the unincorporated [γ-^{32}P]ATP. A fixed amount of labeled Ki-*ras* duplex was mixed with an excess of triple-forming S_i-20AG's in 50 mM Tris-HCl, pH 7.4, 10 mM NaCl, 10 mM $MgCl_2$ (standard buffer) and incubated overnight at 37 °C. After incubation, the mixtures were immediately loaded in a 20% nondenaturing gel prepared in standard buffer and thermostated at 4 °C. After running, the gels were dried under reduced pressure and analyzed on a Phosphorimager (BioRad) in order to determine the relative quantity of radioactivity present in the duplex and triplex bands, for each reaction mixture. DMS/piperidine and DNase I footprintings were performed using the labeled 60-mer target duplex. The labeled duplex (5000 cpm, 12 nM) was incubated overnight with a 500-fold excess of triplex-forming oligonucleotides. After incubation, the DNA samples were either treated with DMS/piperidine or digested with DNase I, as previously described (*16*). The samples were then immediately loaded on a 18% polyacrylamide gel prepared in TBE and 8 M urea, preequilibrated at 55 °C in a Sequi-Gen GT Nucleic Acids Electrophoresis Apparatus (Bio-Rad, Hercules, CA). After running, the gel was dried and exposed to Kodak X-OMAT film, as previously described (*16*).

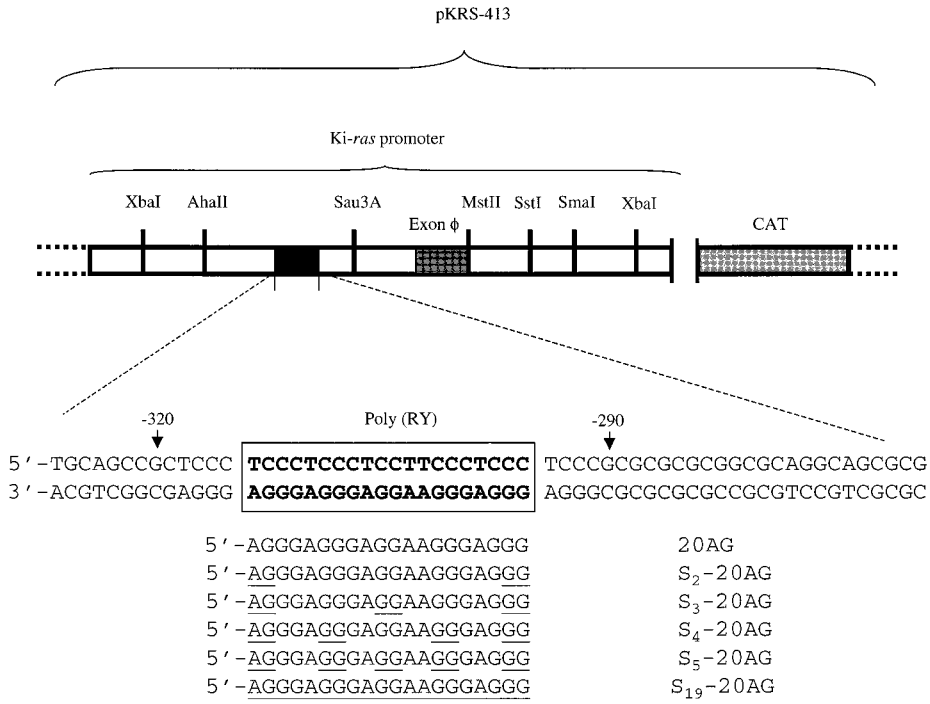

FIGURE 1: Sequence of the unique poly(R·Y) target contained in the murine Ki-*ras* promoter between −320 and −290 from the 3′ boundary of exon ϕ. The triplex-forming AG motif oligonucleotides with an increasing number of phosphorothioate linkages are shown. Oligonucleotide 20AG contains only phosphodiester linkages, and oligonucleotide S_{19}-20AG contained only thioate linkages, whereas oligonucleotides S_i-20AG (i = 2, 3, 4, 5) contained respectively 2, 3, 4, and 5 phosphorothioate backbone linkages. The underlined bases are those linked by a phosphorothioate group. The recombinant plasmid pKRS-413 used to carry out the transient transfection experiments contained the murine Ki-*ras* promoter upstream from the chloramphenicol acetyltransferase (CAT) gene.

Transient Transfection Experiments. Transformed primary human embryonic kidney cell line (293 cells) was cultured in Dulbecco's minimal essential medium containing 10% heat-inactivated fetal calf serum, penicillin (100 units/mL), streptomycin (100 μg/mL), and L-glutamine (2 mM). The day before the transfection, the cells were plated at a density of 7000/cm^2 in 60 mm plates. Cotransfection was carried out by the standard method of calcium phosphate precipitation, using DNA mixtures containing 5 μg of plasmid pKRS-413, 100 ng of pTK-βgal, and 5 μM triplex-forming oligonucleotide. Precipitates were allowed to stand for 45 min without agitation. The precipitates were then added to the cells that were left to stand for 16 h. The medium was replaced, and the cells were left to grow for another 48 h.

CAT and β-Gal Assays. Sixty-four hours after transfection, the cells were washed 3 times with 5 mL of precooled PBS buffer. One milliliter of lysis buffer (MOPS containing 0.1% Triton X-100, pH 6.5) was added, and the cells were left to stand for 30 min. Cell extracts were obtained, and CAT and β-gal assays were performed using commercial CAT and β-gal ELISA kits (Boehringer-Mannheim, Germany). A volume of 200 μL of total proteins extract was incubated in each well of the plate coated with the anti-CAT antibody for 1 h, washed 5 times with washing buffer, and then incubated with anti-CAT antibody conjugated to digoxygenin for 1 h. The plate was washed 5 times and incubated for 1 h with the anti-digoxygenin antibody conjugated to peroxidase enzyme. Finally, 200 μL of the peroxidase substrate was added to the reaction mixture. The reaction catalyzed by peroxidase gave a green color that was quantified by reading the optical density at 405 and 492 nm on a Titertek Multiskan MCC/340 (Labsystem, Finland). A similar procedure was carried out for the β-gal ELISA assay using 200 μL of the same cell extract.

RESULTS

Experimental Design. The promoter of the murine Ki-*ras* gene contains between −290 and −320 from the 3′ boundary of exon ϕ a unique C+G-rich poly(R·Y) sequence which has been demonstrated to be essential for promoter activity, as its deletion yields a dramatic reduction of transcription (*17*). We designed for this target five 20-mer AG motif triplex-forming oligonucleotides, namely, S_i-20AG (i = 2, 3, 4, 5, 19), with an increasing number of nonbridging oxygens replaced with sulfur atoms, as well as a phosphodiester oligonucleotide named 20AG. While S_{19}-ODN contains only phosphorothioate linkages, the oligonucleotides S_i-20AG (i = 2, 3, 4, 5) contain respectively 2, 3, 4, and 5 phosphorothioate linkages distributed in the sequence as shown in Figure 1. The five triplex-forming oligonucleotides S_i-20AG were compared with oligonucleotide 20AG for their ability to bind to the poly(R·Y) target of Ki-*ras* promoter through EMSA and to inhibit, in transfected 293 cells, the expression of the reporter CAT gene placed under the control of the Ki-*ras* promoter. We also compared the behavior of the phosphorothioate oligonucleotides S_i-20AG (i = 2, 3, 4, 5, 19) with that of 20AG as far as their resistance to nucleases and self-association are concerned.

EMSA and Footprinting Experiments. Increasing concentrations of unlabeled triplex-forming S_i-20AG oligonucleotides were incubated overnight at 37 °C with labeled 60-mer Ki-*ras* duplex, in standard buffer. After incubation, the DNA mixtures were run in a thermostated polyacrylamide gel at 4 °C to minimize possible perturbations of the duplex-to-triplex equilibrium. The EMSA profiles obtained with the

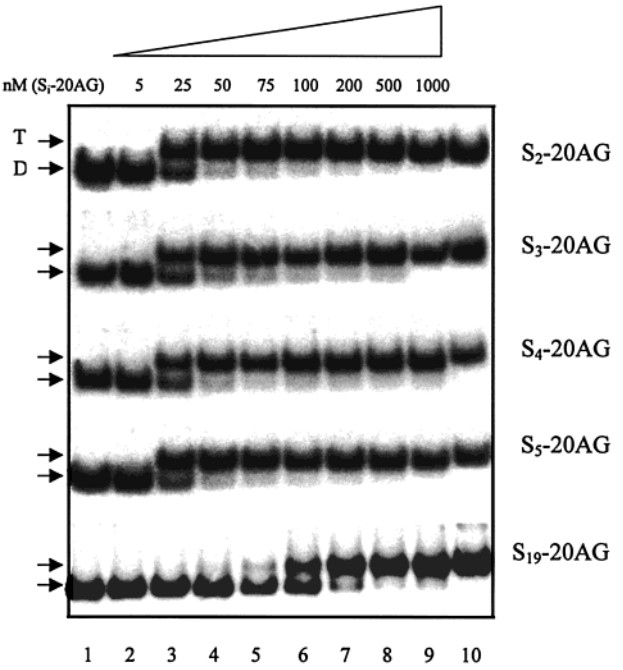

FIGURE 2: EMSA showing triplex formation at the unique poly-(R·Y) target of the Ki-*ras* promoter by the designed oligonucleotides S_i-20AG (i = 2, 3, 4, 5, 19). The reactions were conducted in 50 mM Tris−acetate, pH 7.4, 10 mM NaCl, 10 mM $MgCl_2$. The concentration of the 60-mer duplex was 10 nM; those of each S_i-20AG are shown in the figure. The duplex and triplex species were separated on an 18% polyacrylamide gel run at 4 °C. In lane 1 was loaded a negative control (60-mer duplex plus the 20-mer random-sequence oligonucleotide C_1), while in lane 10 was loaded a positive control (60-mer duplex plus the phosphodiester 20AG oligonucleotide). T and D mean triplex and duplex.

five triplex-forming oligonucleotides S_i-20AG are shown in Figure 2. It can be seen that the phosphorothioates, except S_{19}-20AG, exhibit a duplex-to-triplex transition occurring at the same oligonucleotide concentration of about 25 nM (oligonucleotide:target ratio of 2.5), as we observed for 20AG (not shown). This finding clearly indicates that the presence in 20AG of up to five phosphorothioate linkages (26% backbone modification) does not influence the oligonucleotide binding affinity for the Ki-*ras* sequence. By contrast, S_{19}-ODN exhibits a duplex-to-triplex transition at a higher oligonucleotide concentration, 90 nM. To determine the affinity equilibrium constants, we considered the following duplex-to-triplex equilibrium: D + S_i-20AG ⇔ T. It can be shown that the fraction of triplex contained in the reaction mixture is given by: $f(T) = [S_i\text{-20AG}]/([S_i\text{-20AG}] + K_d)$ (eq a), where K_d is the dissociation constant of the duplex-to-triplex reaction.

Experimental f(T) values as a function of S_i-20AG concentration have been determined by measuring on the Phosphorimager the amount of radioactivity present in the triplex and duplex bands of the electrophoretic profiles. The f(T) versus [S-ODN] plots have been best fitted to eq a by using a nonlinear least-squares program (Sigma Plot, Jandel Scientific Co.) which varied the K_d parameter until the convergence criteria were satisfied. The values of the dissociation constants obtained are collected in Table 1.

The binding between the triplex-forming oligonucleotides S_i-20AG and the Ki-*ras* poly(R·Y) site was also analyzed by DMS and DNase I footprinting experiments. Figure 3A shows the results of a typical experiment in which the

Table 1: Equilibrium Dissociation Constants of Purine Motif Triplexes Containing as Third Strand a Phosphorothioate Oligonucleotide[a]

oligonucleotide[b]	K_d (nM)	ΔG (kJ/mol)
20AG	13 ± 1.0	46.7 ± 3.5
S_2-20AG	12 ± 0.8	46.9 ± 3.1
S_3-20AG	14 ± 1.1	46.5 ± 3.6
S_4-20AG	13 ± 0.9	46.7 ± 3.2
S_5-20AG	10 ± 0.7	47.4 ± 3.3
S_{19}-20AG	128 ± 10.2	40.8 ± 3.2

[a] Data have been obtained in Tris−acetate, pH 7, 10 mM NaCl, 10 mM $MgCl_2$. [b] The sequences of the triplex-forming oligonucleotides are shown in Figure 1.

mixtures containing the 60-mer target duplex and a triplex-forming S_i-20AG were treated at 37 °C with DMS/piperidine. It should be remembered that DMS reacts with G N7 when this position is not involved in hydrogen bonding to the third strand. It can be seen in lanes 3−8 that DMS/piperidine cleavage produces clear footprints exactly in the portion of the 60-mer target duplex where the triplex-forming oligonucleotides S_i-20AG are expected to bind to. At a concentration of 5 μM, the all-thioate oligonucleotide S_{19}-20AG is able to shift completely to the right the duplex-to-triplex equilibrium and to give rise to footprints as strong as those obtained with the oligonucleotides partially modified. Lanes 1, 2, and 9 show that the control oligonucleotides (C_1, C_2, and C_3) do not produce, as expected, a footprint (negative control). Lane 10, by contrast, shows the footprint produced by 20AG (positive control). Figure 3B shows an enzyme protection assay with DNase I. In keeping with the DMS/piperidine experiment, DNase I produces clear footprints with each DNA mixture, thus suggesting that the oligonucleotides S_i-20AG form stable triplexes with the 60-mer target duplex, under similar experimental conditions: standard buffer, 37 °C, S_i-20AG concentration of 1 μM. It can be seen that the all-phosphorothioate S_{19}-20AG protects the 5′-end of the target (gel bottom) from DNase I digestion slightly less efficiently than the other oligonucleotides S_i-20AG, in accord with the fact that S_{19}-20AG shows a lower affinity for the target with respect to oligonucleotides S_i-20AGs (i = 2, 3, 4, 5).

Oligonucleotide Self-Aggregation and Resistance to S1 Nuclease. To gain insight into the solution properties of the triplex-forming oligonucleotides S_i-20AG, we examined their electrophoretic mobility as a function of oligonucleotide concentration. The triplex-forming oligonucleotides were dissolved in 50 mM Tris−acetate, pH 7.4, 150 mM KCl, 10 mM $MgCl_2$ at the concentrations of 50 nM and 5 μM. Both DNA solutions were first heated at 90 °C for 5 min and then incubated overnight at 37 °C. After incubation, the DNA mixtures were analyzed in a native polyacrylamide gel, thermostated at 4 °C. Figure 4A shows that S_i-20AGs migrated with three bands which we attributed to single-strand (B_0), dimer (B_1), and tetraplex (B_2) structures (*18*−*21*), formed by self-association. At 50 nM (low concentration), all-phosphodiester 20AG migrated as single strand and tetraplex, whereas the phosphorothioate S_i-20AG analogues mainly adopted a single-strand form, but also, in small proportion, some multistrand structures (dimer and tetraplex) whose amounts depended on the number of phosphorothioate linkages present in the oligonucleotide sequence. In contrast, oligonucleotide S_{19}-20AG migrated at 50 nM as single strand

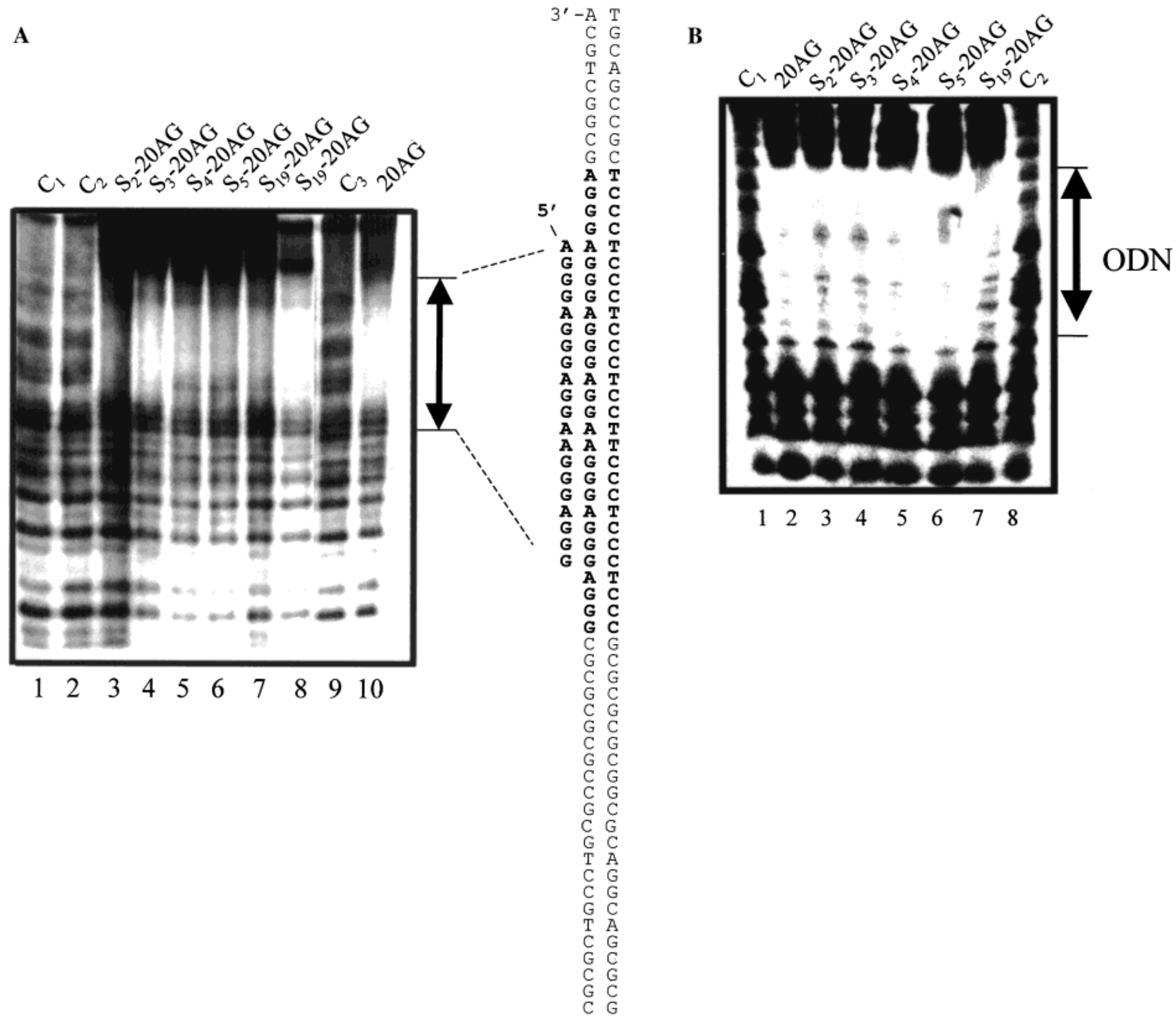

FIGURE 3: Footprinting experiments. (A) DMS/piperidine footprinting carried out in 50 mM Tris−acetate, pH 7.4, 10 mM $MgCl_2$, 37 °C, showing the binding of oligonucleotides S_i-20AG (i = 2, 3, 4, 5, 19) (5 μM) and 20AG to the 60-mer target duplex (10 nM) containing the poly(R·Y) sequence of Ki-*ras*. Oligonucleotides C_1 (20-mer oligonucleotide without thioate linkages), C_2 (34-mer oligonucleotide with 6 thioate linkages), and C_3 (34-mer oligonucleotide with 12 thioate linkages) are negative control oligonucleotides with a random sequence which have been proved to be unable to bind to the Ki-*ras* target via triple helix formation. (B) DNase I footprinting showing the interaction between the 60-mer K_i-*ras* target (10 nM) and oligonucleotides S_i-20AG (i = 2, 3, 4, 5, 19) and 20AG (5 μM). Lanes 1 and 8 show the digestion profiles obtained in the presence of control oligonucleotides C_1 and C_2.

and dimer. By increasing the oligonucleotide concentration, the intermolecular interactions and thus the formation of multistrand structures by self-association were favored. At 5 μM (high concentration), oligonucleotides S_i-20AG (i = 2, 3, 4, 5) and 20AG were found to migrate as dimer (B_1) and tetraplex (B_2), wheras S_{19}-20AG migrated mainly as a dimer and, in a very low amount, as a tetraplex. As observed at lower concentration, the phosphorothioate linkages destabilize the tetraplex structure. Indeed, under the experimental conditions adopted, it was found that the full thioate S_{19}-20AG hardly form tetraplex stuctures.

The oligonucleotide aggregation was also investigated by circular dichroism (CD) measurements. All S_i-20AG oligonucleotides at 3 μM showed CD spectra characterized by a strong and positive ellipticity band at 260 nm whose intensity decreased as a function of temperature. Typical spectra for S_{19}-20AG and S_3-20AG are shown in Figure 4B,C. The shape of the spectra and the dependence of their intensity on temperature indicated that the oligonucleotide self-associated in dimer and tetraplex structures (*22*, *23*). Plotting the CD signal (260 nm) against the temperature, we obtained melting curves indicating that S_i-20AG (i = 2, 3, 4, 5) denature in a noncooperative manner, a behavior suggesting that oligonucleotides S_i-20AG adopt in solution more than one structure (B_1 and B_2). In contrast, oligonucleotide S_{19}-20AG exhibits a more cooperative melting profile with a T_m of 45 °C. As S_{19}-20AG migrates with only one electrophoretic band at micromolar concentrations, it should adopt, in solution, a duplex form and not a stiff single-strand conformation of low mobility (*24*).

The resistance of 20AG and S_i-20AG (i = 2, 3, 4, 5, 19) to S1 nuclease was investigated by measuring at 260 nm the absorbance as a function of time, after the oligonucleotides were exposed to the nuclease (*8*). The oligonucleotide degradation is accompanied by an hyperchromic effect that increases as a function of time. Figure 5 show the digestion curves from which it can be seen that the half-life of oligonucleotides S_i-20AG (3 μM) increases with the number of phosphorothioates present in the oligonucleotide sequence. After 1 h of digestion, the phosphodiester 20AG oligonucleo-

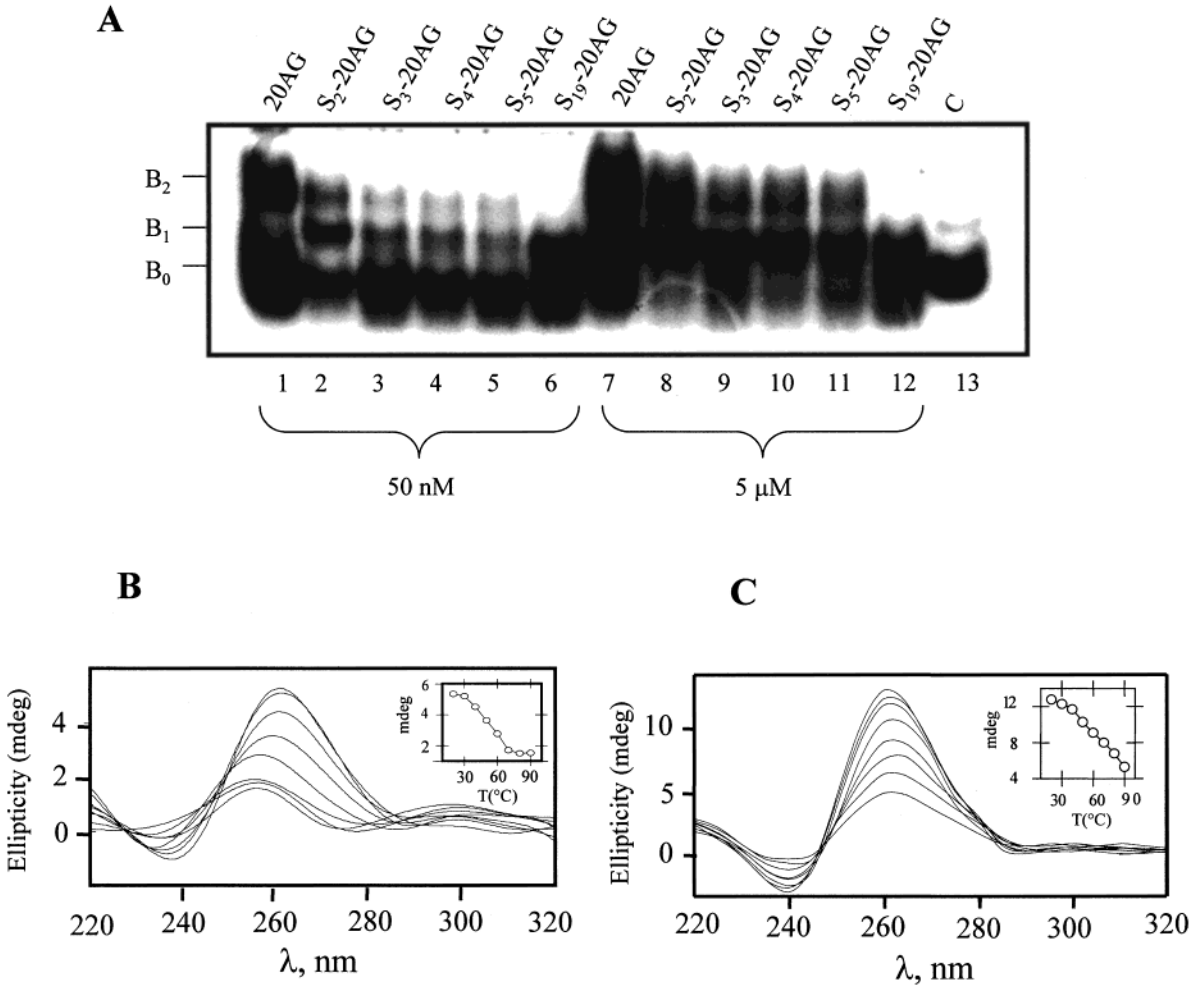

FIGURE 4: (Panel A) Electrophoresis analysis in 50 mM Tris−acetate, pH 7.4, 150 mM KCl, 10 mM $MgCl_2$ of 20AG and phosphorothioate oligonucleotides S_i-20AG (i = 2, 3, 4, 5, 19) at low (50 nM, lanes 1−6) and high (5 μM, lanes 7−12) concentrations. The electrophoretic run was performed at 4 °C. The oligonucleotides assume in solution three DNA species which we believe to be single strand (B_0), dimer (B_1), and tetraplex (B_2) structures. Lane 13 shows the mobility of a 21-mer oligonucleotide of random sequence. (Panels B and C) Circular dichroism spectra as a function of temperature of S_{19}-20AG (panel B) and S_3-20AG (panel C). Spectra have been obtained in 50 mM Tris−acetate, pH 7.4, 10 mM NaCl, 10 mM $MgCl_2$. The spectra report on the ordinate the ellipticity in millidegree units. The oligonucleotide concentration was 3 μM.

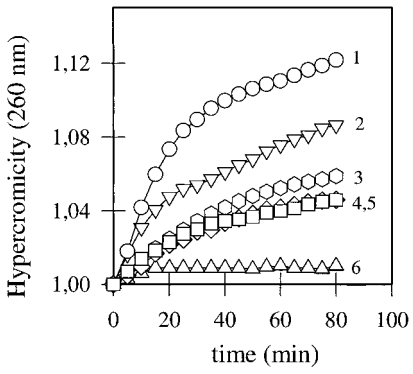

FIGURE 5: S1 digestion of S_i-20AGs as a function of time. The absorbance at 260 nm of DNA solutions containing 0.02 μg/mL oligonucleotide and 7.5 units/mL S1 nuclease was recorded as a function of time. Oligonucleotides 20AG (curve 1), S_2-20AG (curve 2), S_3-20AG (curve 3), S_4-20AG (curve 4), S_5-20AG (curve 5), and S_{19}-20AG (curve 6).

tide is completely degraded, whereas 60% of the phosphorothioate S_3-20AG is still in the full-length form.

Transfection Experiments in 293 Cells. The inhibitory capacity of the triplex-forming oligonucleotides S_i-20AG (i = 2, 3, 4, 5, 19) was examined by cotransfecting the 293 cells with the recombinant vector pKRS-413, containing the CAT gene downstream from the Ki-*ras* promoter (*13*), with triplex-forming S_i-20AG oligonucleotides (Figure 1). In the transfection mixture, we also added plasmid pTK β-gal to evaluate the transfection efficiency. To quantitatively measure both CAT and β-gal expressions, we performed CAT and β-gal ELISA immunoassays with commercial anti-CAT and anti-β-gal polyclonal antibodies (Boehringer Mannheim, Germany). We first transfected the 293 cells with pKRS-413 and pTK-βgal at different concentrations in order to find out the plasmid ratio which gives a comparable ELISA response in terms of optical density. We found that when pKRS-413 was in the microgram and pTK-βgal in the nanogram range, the immunoassay response that they elicited was of the same order and linear over a time range of 50 min, as shown in Figure 6. As control experiments, we transfected 293 cells only with pKRS-413 and with pKRS-413 together with a random-sequence oligonucleotide which is unable to form a triplex with the poly(R·Y) sequence of c-Ki-*ras* (as control we used a 20-mer phosphodiester, C_1, and two 34-mer phosphorothioates, C_2 and C_3, random-

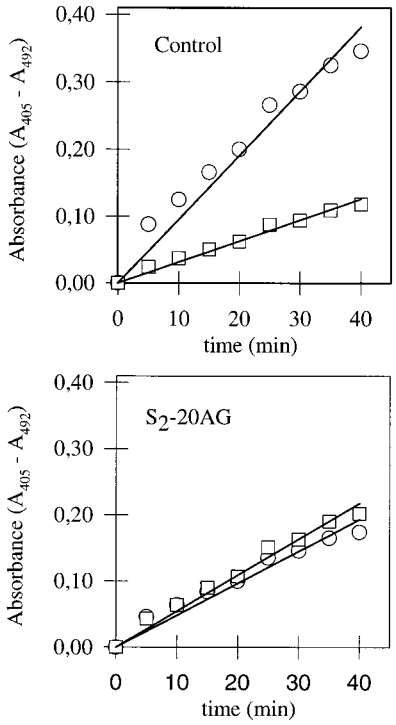

FIGURE 6: Colorimetric CAT (○) and β-gal (□) immunoassays for the quantitative determination of CAT and β-gal expression in transfected 293 cells. The assay is based on the sandwich ELISA principle (Boehringer Mannheim, Germany). The absorbance difference ($A_{405} - A_{492}$) relative to CAT and β-gal expression was read on a microtiter plate reader at several intervals and plotted as a function of time. The top panel shows a control experiment: i.e., CAT and β-gal expression obtained when cotransfecting the cells with pKRS-413, pTK-βgal, and a random-sequence oligonucleotide (C_1 or C_2 or C_3). The bottom panel shows CAT and β-gal expression obtained when cotransfecting the cells with pKRS-413, pTK-βgal, and the triplex-forming oligonucleotide S_2-20AG. The absorbance difference ($A_{405} - A_{492}$) of the samples is directly correlated to the levels of CAT and β-gal and thus to the expression of the relative genes. Note that the phosphorothioate S_2-20AG oligonucleotide promotes a significant inhibition of CAT expression.

sequence oligonucleotides containing, respectively, 6 and 12 phosphorothioate linkages, which are unable to form triple helices with the Ki-*ras* target). The results of four independent transfection experiments are shown in the histograms shown in Figure 7. These data have been obtained by determining for each transfection the value of the CAT:β-gal ratio, obtained transfecting the cells with a DNA mixture containing pKRS-413, pTK-βgal, and a triplex-forming oligonucleotide S_i-20AG. The CAT:β-gal ratio was then normalized for the control, i.e., the average ratio obtained transfecting the cells with pKRS-413, pTK-βgal, and a control oligonucleotide (C_1 or C_2 or C_3). It can be seen that oligonucleotides S_i-20AG promote a selective and strong repression of CAT expression up to 75%. The data seem to indicate that the CAT inhibition promoted by the phosphorothioate oligonucleotides is stronger than that observed with the 20AG phosphodiester analogue. The molecular basis of this behavior is discussed in the next section.

DISCUSSION

This study characterizes both binding and anti-gene properties of a number of triplex-forming oligonucleotides containing increasing levels of phosphorothioate linkages. The designed S_i-20AG oligonucleotides are expected to bind

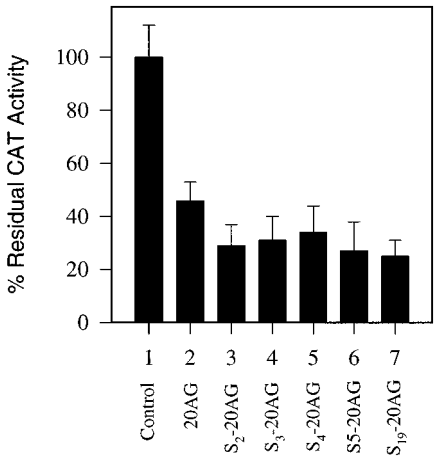

FIGURE 7: Anti-gene activity of the anti-gene oligonucleotides S_i-20AG. Data are plotted as percent residual CAT expression from the reporter plasmid pKRS-413 defined as the CAT/β-gal from cells transfected with one triplex-forming oligonucleotide S_i-20AG (i = 2, 3, 4, 5, 19) or 20AG, normalized by CAT/β-gal from cells transfected with a control oligonucleotide (C_1 or C_2 or C_3). Note that the phosphorothioate triplex-forming oligonucleotides promote a strong inhibition of CAT expression of up to 75%.

to the major groove of a critical Ki-*ras* poly(R·Y) sequence in the antiparallel orientation, forming reverse-Hoogsteen A·AT and G·GC base triplets (*25*−*27*). EMSA experiments show that replacing up to five phosphodiester groups with phosphorothioates in the all-phosphodiester 20AG oligonucleotide does not change the equilibrium dissociation constant, which has been found to be about 12 ± 2 nM. Previously we reported for 20AG a K_d of 37 nM, which is higher than the value reported here (*13*). However, if one considers that the experiments have been performed in different salts: 50 mM NaCl, 5 mM $MgCl_2$ versus 10 mM NaCl, 10 mM $MgCl_2$ (this study), this difference is to be expected (*28*−*30*). By contrast, all-thioate S_{19}-20AG exhibits a K_d higher by one order of magnitude, i.e., 120 ± 15 nM. This finding is somewhat in contrast with the literature data according to which phosphorothioate modifications to purine triplex-forming oligonucleotides should not significantly reduce the oligonucleotide affinity to duplex DNA (*10*, *11*). In contrast, when the triplex-forming oligonucleotide has a pyrimidine motif, the triplex stability depends more markedly on the number of sulfur atoms introduced in the third strand. We previously found that the substitution in the sugar−phosphate backbone of 5′-CTTCCTCCTCT with an increasing number of phosphodiester or phosphorothioate linkages resulted in a gradual decrease of the triplex T_m from 42 to 31 °C. On average, the T_m was reduced by 2 °C for each thioate group introduced in the 11-mer oligonucleotide (*8*). Why does a sulfurized third strand produce different effects on parallel and antiparallel triplexes? To answer this question, one should keep in mind that: (a) in antiparallel triplexes the purine third strand lies practically in the middle of the major groove of the target duplex, while in parallel triplexes the pyrimidine third strand lies close to the purine strand of the target (*31*); (b) sulfur has a larger van der Waal's radius than oxygen (1.85 versus 1.44 Å) and a lower electronegativity (2.5 versus 3.5 on the Pauling scale); (c) sulfur is more polarizable than oxygen, according to Raman and IR studies (*32*). Thus, while in the phosphodiester group the negative charge is delocalized over the two oxygens, in a phospho-

rothioate group it should lie on the sulfur. A sulfurized third strand can destabilize a triplex mainly by two ways: (a) the sulfur atoms may alter the counterion condensation of the triplex; (b) the anion−anion repulsion between fully negative sulfurs and partly negative oxygens juxtaposed in the major groove should increase. According to this structural model, it is not surprising that the affinity of all-thioate S_{19}-20AG for the Ki-*ras* target is 1 order of magnitude lower than those observed with the partially sulfurized S_i-20AG third strands. This interpretation of the binding data is supported by the observation that a triplex-forming S-ODN in the S_p configuration, whose sulfur atoms lie on the side of the purine strand of the target duplex, forms a triplex less stable than the triplex formed by the analogue R_p isomer (*33*).

A nondelocalized negative charge in thioate linkages seems to have a significative effect also on the aggregation of the designed triplex-forming S_i-20AGs. Figure 4 shows that all-phosphodiester 20AG self-associates into a tetraplex even at low concentration (50 nM). At high concentration (5 μM), 20AG self-associates into both dimer and tetraplex species, suggesting that the tetraplexes are more stable than the dimer. Interestingly, phosphorothioate oligonucleotides S_i-20AG do not exhibit such a behavior. At both low and high concentrations, they do not easily form aggregated structures such as tetraplexes, probably because the anion−anion repulsions in the tetraplexes formed by the phosphorothioate oligonucleotides S_i-20AG are higher than the repulsions present in the tetraplex formed by the phosphodiester 20AG. As expected, Figure 4 shows that the higher the number of sulfur atoms contained in the oligonucleotide, the lower will be the propensity to form tetraplex structures. When the oligonucleotide contains all-thioate groups such as S_{19}-20AG, it does not practically form tetraplex structures. From these data, we may conclude that S_i-20AG, containing only 20% of phosphorothioate groups, exhibit a significantly lower tendency to form tetraplex structures as compared to the phosphodiester analogues.

Phosphorothioate oligonucleotides are not easily cleavable by many enzymes. The molecular basis of their nuclease resistance is not yet well understood. Recent studies, however, have suggested that the sulfur atoms may inactivate the nucleases by displacing the metal ions from the active center of the enzymes (*34*, *35*). The S1 digestion curves for the S_i-20AG oligonucleotides, in combination with the binding and aggregation data, suggest a guideline for the rational design of anti-gene phosphorothioate with the AG motif. It is sufficient to introduce three or four phosphorothioate linkages in a 20-mer oligonucleotide such as 20AG to make the oligonucleotide resistant to nucleases and incapable of aggregating in solution, without reducing its binding affinity to duplex DNA.

Transient transfection experiments showed that the designed triplex-forming oligonucleotides S_i-20AG are stronger repressors of CAT expression by the reporter construct than the phosphodiester 20AG (*13*). In particular, oligonucleotides S_5-20AG and S_{19}-20AG seem to have higher anti-gene capacity (25 ± 7% and 27 ± 11% residual CAT expression, respectively). These in vivo assays were performed by incubating before transfection the reporter pKRS-413 plasmid containing CAT under the control of the Ki-*ras* promoter with a specific S_i-20AG oligonucleotide. In such a way, the triplex was preformed in vitro and then transfected into 293 cells with the calcium phosphate technique. It is found that S_{19}-20AG, although having a lower binding capacity, seems to produce a stronger anti-gene effect with respect to 20AG. To rationalize this observation, one may consider that inside the cell the oligonucleotides bound to the plasmid undergo a bound−unbound equilibrium with the target. However, when the triplex-forming oligonucleotides are in the unbound state, they are subject to degradation by endogenous nucleases to an extent that depends on the chemical nature of the oligonucleotide backbone. As 20AG is more susceptible to nuclease digestion than S_{19}-20AG and exhibits a stronger tendency to aggregate into stable tetraplex structures, it shows a lower anti-gene capacity than that observed for the fully and partly thioate analogues.

In conclusion, the data presented in this study provide a guide for designing anti-gene effector molecules for the selective inhibition of chromosomal genes. Contrary to pyrimidine triplex-forming phosphorothioate oligonucleotides, the AG motif analogues do not reduce their ability to bind to duplex DNA if only 20−30% of their phosphodiester backbone groups are replaced by phosphorothioate linkages. Moreover, a partial backbone modification not only makes the S_i-20AG anti-gene effectors more stable against S1 nuclease but also reduces significantly the oligonucleotide tendency to aggregate into high molecular weight structures. This is not the only strategy we used to inhibit the Ki-*ras* promoter. Recently, we obtained about 50% inhibition of the CAT gene driven by Ki-*ras* promoter by using recombinant expression vectors which were able, once transfected in the cells, to generate intracellularly short RNA transcripts, with the same sequence of 20AG, capable of binding to the poly(R·Y) site of Ki-*ras* via triple helix formation (*36*).

ACKNOWLEDGMENT

We thank Igor Paron and Chiara Suraci for electrophoretic experiment assistance, and N. Yathindra for critical reading of the manuscript

REFERENCES

1. Wagner, R. W. (1995) *Nat. Med. 1*, 1116−1118.
2. Galderisi, U., Cascino, A., and Giordano, A. (1999) *J. Cell. Physiol. 181*, 251−257.
3. Vasquez, K. M., and Wilson, J. H. (1998) *Trends Biochem. Sci. 23*, 4−9.
4. Hélène, C., Giovannangeli, C., Guieysse-Peugeot, A. L., and Praseuth, D. (1997) *Ciba Found. Symp. 209*, 94−106.
5. Latimer, L. J., Hampel, K., and Lee, J. S. (1989) *Nucleic Acids Res. 17*, 1549−1561.
6. Kibler-Herzog, L., Zon, G., Uznanski, B., Wittier, G., and Wilson, W. D. (1991) *Nucleic Acids Res. 19*, 2979−2986.
7. Kim, S.-G., Tsukahara, S., Yoyama, S., and Takaku, H. (1992) *FEBS Lett. 314*, 29−32.
8. Xodo, L., Alunni-Fabbroni, M., Manzini, G., and Quadrifoglio, F. (1994) *Nucleic Acids Res. 22*, 3322−3330.
9. Hacia, J. G., Wold, B. J., and Dervan, P. B. (1994) *Biochemistry 33*, 5367−5369.
10. Joseph, J., Kandala, J. C., Veerapanane, D., Weber, K. T., and Guntaka, R. V. (1997) *Nucleic Acids Res. 25*, 2182−2188.
11. Kim, H. G., Reddoch, J. F., Mayfield, C., Ebbinnghaus, S., Vigneswaran, N., Thomas, S., Jones, D. E., Jr., and Miller, D. M. (1998) *Biochemistry 37*, 2299−2304.
12. Alunni-Fabbroni, M., Manfioletti, G., Manzini, G., and Xodo, L. (1994) *Eur. J. Biochem. 226*, 831−839.

13. Alunni-Fabbroni, M., Pirulli, D., Manzini, G., and Xodo, L. (1966) *Biochemistry 35*, 16361−16369.
14. Sambroook, J., Fritsch, E. F., and Maniatis, T. (1989) *Molecular cloning: a laboratory manual*, Cold Spring Harbor Press, Cold Spring Harbor, NY.
15. Hoffman, E. K., Trusko, S. P., Freeman, N., and George, D. L. (1987) *Mol. Cell. Biol. 7*, 2592−2596.
16. Xodo, L., Manzini, G., and Quadrifoglio, F. (1998) *Antisense Nucleic Acid Drug Dev. 8*, 477−488.
17. Hoffman, E. K., Trusko, S. P., Murphy, M., and George, D. L. (1990) *Proc. Natl. Acad. Sci. U.S.A. 87*, 2705−2709.
18. Guschlbauer, W., Chantot, J.-F., and Thiele, D. (1990) *J. Biomol. Struct. Dyn. 8*, 491−511.
19. Hardin, C. C., Henderson, E., Watson, T., and Prosser, J. K. (1991) *Biochemistry 30*, 4460−4472.
20. Rhodes, D., and Giraldo, R. (1995) *Curr. Opin. Struct. Biol. 5*, 311−322.
21. Lee, J. S. (1990) *Nucleic Acids Res. 18*, 6057−6060.
22. Rippe, K., Fritsch, V., Westhof, E., and Jovin, T. M. (1992) *EMBO J. 11*, 3777−3786.
23. Vorlickova, M., Zimulova, M., Kovanda, J., Fojtik, P., and Kypr, J. (1998) *Nucleic Acids Res. 26*, 2679−2685.
24. Morassutti, C., Scaggiante, B., Dapas, B., Xodo, L., Tell, G., and Quadrifoglio, F. (1999) *Biochimie 81*, 1−8.
25. Fox, K. R. (2000) *Curr. Med. Chem. 7*, 17−37.
26. Doronina, S. O., and Behr, J. P. (1997) *Chem. Soc. Rev. 26*, 63−71.
27. Beal, P. A., and Dervan, P. B. (1991) *Science 251*, 1360−1363.
28. Singleton, S. F., and Dervan, P. B. (1993) *Biochemistry 32*, 13171−13179.
29. Floris, R., Scaggiante, B., Manzini, G., Quadrifoglio, F., and Xodo, L. E. (1999) *Eur. J. Biochem. 260*, 801−809.
30. Blume, S. W., Leibowitz, J., Zacharias, W., Guarceló, V., Mayfield, C. A., Ebbinghaus, S. W., Bates, P., Jones, D. E., Jr., Trent, J., Vigneswaran, N., and Miller, D. M. (1999) *Nucleic Acids Res. 27*, 695−702.
31. Radhakrishnan, I., and Patel, D. J. (1993*) Structure 1*, 135−152.
32. Frey, P. A., and Sammons, R. D. (1985) *Science 228*, 541−545.
33. Kim, S. G., Tsukahara, S., Yokoyama, S., and Takaku, H. (1992) *FEBS Lett. 314*, 29−32.
34. Eckstein, F. (2000) *Antisense Nucleic Acid Drug Dev. 10*, 117−121.
35. Brautigam, C. A., and Steitz, T. A. (1998) *J. Mol. Biol. 277*, 363−377.
36. Cogoi, S., Suraci, C., Diviacco, S., Del Terra, E., van der Marel, G., Quadrifoglio, F., and Xodo L. (2000) *Antisense Nucleic Acid Drug Dev. 10*, 283−295.

BI0012639